Performance Analysis of Sliding Mode Control for Real-time Hybrid Test

B. Wu & H. Zhou
School of Civil Engineering, Harbin Institute of Technology,
Huanghe Road, No. 73, Harbin 150090, China

SUMMARY:
The equivalent force control method uses feedback control to replace a mathematical iteration required to solve the nonlinear equation of real-time hybrid test with an implicit integration method. The commonly used PID controller as a candidate of equivalent force control has only limited robustness for nonlinear systems. For the nonlinear specimen in a real-time hybrid test, the sliding mode control is proposed to be used as the outer-loop controller of the equivalent force control. The design method of sliding mode control for equivalent force control is presented. The effects of key parameters of sliding mode controller on the performance of equivalent force control with are discussed and demonstrated through numerical simulation.

Keywords: Real-time Hybrid test; Equivalent force control method; Sliding mode control; Nonlinear

1. INTRODUCTION

The real-time substructure testing (RSTing) divides the structure into two parts: the critical element is taken as experimental substructure and the remainder of the structure is a numerical model in computer. It can be used to test with large-scale or even full-scale specimens the dynamic performance of a structure accurately [Williams et al. (2001)].

In real-time substructure test, the integration method is critical to the success of the test. The explicit integration method such as the central difference method (CDM)(Wu et al. 2005) is usually conditionally stable. Although unconditionally stable explicit methods[Chen and Ricles (2008) and Bursi et al. (2008)] are available, all these methods require the information of structures; the stability and accuracy may be worsened if the structure enters nonlinear range. In contrast, most implicit methods (Jung, 2007) possess unconditional stability and good accuracy for nonlinear systems, but they demand complicated iteration to solve the nonlinear difference equation. Wu et al. (2007) proposed the equivalent force control (EFCM) method in which the nonlinear equation of implicit integration is solved by a so-called *equivalent force* feedback control. The PID controller has been used for equivalent force control (Wu, 2011). But, as the PID is a linear controller, it has only limited robustness for nonlinear systems. So the nonlinear control methods are preferred in tests with nonlinear specimens.

The sliding mode control (SMC) also named variable structure control is a nonlinear control method. Recently, it has been applied in structural control and structural testing system control. Yang et al. (1995) firstly applied the sliding mode control in structural control. The numerical simulation results showed that it has good control effect for nonlinear and hysteretic structures. Wang et al. (2007) applied the sliding mode control method to control the actuator in real-time substructure test. The numerical simulations showed that sliding mode has better performance than PID control for nonlinear specimens.

In this study, the sliding mode control is proposed as the equivalent force controller for real-time hybrid testing. We will discuss the controller design and chattering problem. Results of numerical simulation will be given to demonstrate the performance of the sliding mode control.

2. OVERVIEW OF EFCM

In order to study the EFC method with SMC, the formulation of EFC (Wu, 2011) is introduced first. The equation of the motion for a RST at step i+1 can be expressed in a time-discretized form as

$$\mathbf{M}_{\mathrm{N}}\boldsymbol{a}_{i+1}+\mathbf{C}_{\mathrm{N}}\boldsymbol{v}_{i+1}+\mathbf{R}_{\mathrm{N}}(\boldsymbol{d}_{i+1})+\mathbf{R}_{\mathrm{E}}(\boldsymbol{a}_{i+1},\boldsymbol{v}_{i+1},\boldsymbol{d}_{i+1})=\mathbf{F}_{i+1} \tag{2.1}$$

in which, **M** and **C** are the mass and damping matrices; **R** is the restoring force vector; ***d***, ***v*** and ***a*** are the displacement, velocity and acceleration vectors of the structure, respectively; **F** is the excitation force vector; the subscript N denotes variables associated with the numerical substructure, and the subscript E denotes variables associated with the experimental substructure.

With the Newmark constant-average-acceleration method, the acceleration and velocity are expressed in terms of displacement at the (i +1) step as

$$\boldsymbol{a}_{i+1}=\frac{4}{\Delta t^2}(-\boldsymbol{d}_i-\Delta t\boldsymbol{v}_i-\frac{\Delta t^2}{4}\boldsymbol{a}_i+\boldsymbol{d}_{i+1}) \tag{2.2}$$

$$\boldsymbol{v}_{i+1}=-\frac{2}{\Delta t}\boldsymbol{d}_i-\boldsymbol{v}_i+\frac{2}{\Delta t}\boldsymbol{d}_{i+1} \tag{2.3}$$

in which Δt is the integration time interval. Substituting Eqns. 2.2. and 2.3. into Eqn. 2.1. gives

$$\mathbf{R}_{\mathrm{N}}(\boldsymbol{d}_{i+1})+\mathbf{K}_{\mathrm{PD}}\boldsymbol{d}_{i+1}+\mathbf{R}_{\mathrm{E}}(\boldsymbol{a}_{i+1},\boldsymbol{v}_{i+1},\boldsymbol{d}_{i+1})=\mathbf{F}_{\mathrm{EQ},i+1} \tag{2.4}$$

in which $\mathbf{K}_{\mathrm{PD}}=\frac{4\mathbf{M}_{\mathrm{N}}}{\Delta t^2}+\frac{2\mathbf{C}_{\mathrm{N}}}{\Delta t}$ (2.5)

$$\mathbf{F}_{\mathrm{EQ},i+1}=\mathbf{F}_{i+1}+\mathbf{M}_{\mathrm{N}}\boldsymbol{a}_i+(\frac{4\mathbf{M}_{\mathrm{N}}}{\Delta t}+\mathbf{C}_{\mathrm{N}})\boldsymbol{v}_i+(\frac{4\mathbf{M}_{\mathrm{N}}}{\Delta t^2}+\frac{2\mathbf{C}_{\mathrm{N}}}{\Delta t})\boldsymbol{d}_i \tag{2.6}$$

In the above equations, $\mathbf{K}_{\mathrm{PD}}$ is called pseudodynamic stiffness; $\mathbf{F}_{\mathrm{EQ},i+1}$ can be considered as an equivalent force command consisting of the external force as well as the pseudodynamic effect that depends only on the previous step response. Eqn. 2.4. can be viewed as a hybrid dynamic equilibrium condition.

An RST with the EFC method is illustrated by the block diagram in Fig. 2.1. In the Figure, two controllers are shown. The inner one is for traditional displacement control of actuator-specimen system. The outer one is for equivalent force control that is used to enforce the equilibrium condition presented in Equation. 2.4. In each time interval Δt, the force error e_{EQ} between the equivalent force command $\mathbf{F}_{\mathrm{EQ},i+1}(t)$ and the response $\mathbf{F}'_{\mathrm{EQ},i+1}(t)$, is converted to a displacement command $\boldsymbol{d}^{c}_{i+1}(t)$ using a force controller and a conversion matrix $\mathbf{C}_{\mathrm{F}}$. The terms $\mathbf{R}_{\mathrm{E}}[\boldsymbol{d}'_{i+1}(t)]$ and $\boldsymbol{d}'_{i+1}(t)$ are the restoring force and displacement response of the experimental substructure subjected to the command $\boldsymbol{d}^{c}_{i+1}(t)$, respectively. If the equivalent force response closely tracks the command by force controller, the displacement command $\boldsymbol{d}^{c}_{i+1}(t)$ should approach the actual displacement solution $\boldsymbol{d}_{i+1}$. The matrix $\mathbf{C}_{\mathrm{F}}$ can be set to a constant value and be constructed with the partial derivatives of the left-hand side of Equation. 2.4. with respective to $\boldsymbol{d}_{i+1}$ at the initial state of the test structure.

3. DESIGN OF CONTROLLER

For controller design, a numerical model of the plant, *i.e.*, the actuator-specimen system, is needed. In general, an actuator attaching a nonlinear specimen is a nonlinear system, which includes nonlinearities both from the specimen and from the actuator such as square root relationship between

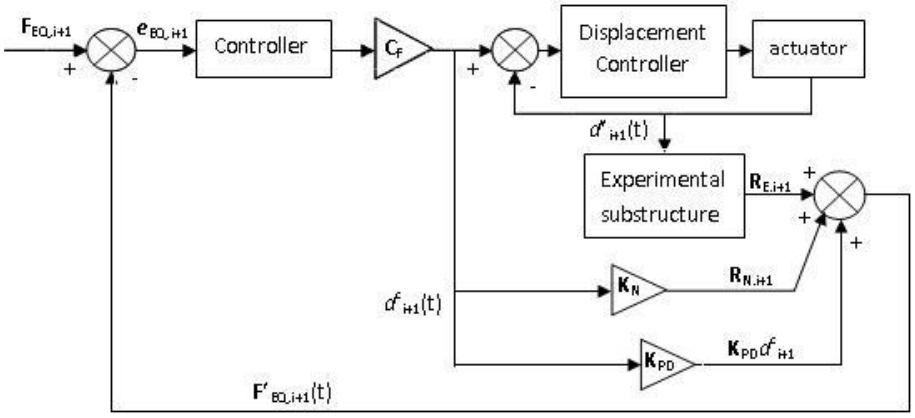

Figure 2.1. Block diagram of EFC

oil pressure and flow, and oil leakage effects [Williams et al.(2001)]. However, when the capacity of the actuator is much larger than the resistance force of the specimen, the actuator system may be simply approximated by a linear system. A Second-order linear actuator model considering the effect of the variable stiffness of the specimen is used here, which, for convenience of later analysis, is expressed in time domain as

$$\frac{\mathrm{d}^2}{\mathrm{d}t^2}d^m + a_1\frac{\mathrm{d}}{\mathrm{d}t}d^m + a_2 d^m + a_3\frac{\mathrm{d}^2}{\mathrm{d}t^2}r_E + a_4\frac{\mathrm{d}}{\mathrm{d}t}r_E = b_1\frac{\mathrm{d}}{\mathrm{d}t}d^c + b_2 d^c \tag{3.1}$$

in which $a_1 = \dfrac{K_P k_0 \beta_E}{(2\beta_E + P)A_P}$, $a_2 = \dfrac{K_i k_0 \beta_E}{(2\beta_E + P)A_P}$, $a_3 = \dfrac{2V}{(2\beta_E + P)}$, $a_4 = \dfrac{K_{\Delta P}\beta_E}{(2\beta_E + P)A_P^2}$, $b_1 = \dfrac{K_P k_0 \beta_E}{(2\beta_E + P)A_P}$ and $b_2 = \dfrac{K_i k_0 \beta_E}{(2\beta_E + P)A_P}$; d^c and d^m are displacement commands and responses; K_P and K_I are the displacement controller parameters; r_E is the resistance force of the specimen; k_o is a gain factor that relates the rate of the total oil flow q_t into and out of the actuator chambers and the spool displacement x_s; V is the volume of chamber; β_E is the effective bulk modulus of oil; A_P is the piston area; P is the supply oil pressure; $K_{\Delta P}$ is a gain factor for delta pressure feedback.

For convenience, we denote as the plant the assemblage of actuator, experimental and numerical substructures, pseudodynamic stiffness and force-displacement conversion factor. For a linear single degree of freedom (SDOF) structure, the plant is described by

$$\frac{\mathrm{d}^2 F_{EQ}^m}{\mathrm{d}t^2} + a_1\frac{\mathrm{d}F_{EQ}^m}{\mathrm{d}t} + a_2 F_{EQ}^m + a_3'\frac{\mathrm{d}^2 r_E}{\mathrm{d}t^2} + a_4'\frac{\mathrm{d}r_E}{\mathrm{d}t} + a_5' r_E = u_e \tag{3.2}$$

in which $a_3' = a_3(K_N + K_{PD}) - 1$, $a_4' = a_4(K_N + K_{PD}) - a_1$, $a_5' = -a_2$, $u_e = b_1'\dfrac{\mathrm{d}u}{\mathrm{d}t} + b_2' u$, $b_2' = b_2 C_F(K_N + K_{PD})$ and $b_1' = b_1 C_F(K_N + K_{PD})$. By defining

$$\mathbf{X} = \begin{Bmatrix} x_1 \\ x_2 \end{Bmatrix} = \begin{Bmatrix} F_{EQ}^m \\ \dot{F}_{EQ}^m \end{Bmatrix} \tag{3.3}$$

The state-space model of the plant can be obtained as

$$\begin{cases} \dot{\mathbf{X}} = \mathbf{AX} + \mathbf{B}(u_e + f) & (3.4a) \\ F_{EQ}^m = \mathbf{CX} & (3.4b) \end{cases}$$

where $\mathbf{A}=\begin{bmatrix} 0 & 1 \\ -a_2 & -a_1 \end{bmatrix}$, $\mathbf{C}=[1\ \ 0]$, $\mathbf{B}=[0\ \ 1]^{\mathrm{T}}$, $f = a_3' \dfrac{d^2}{dt^2} r_E + a_4' \dfrac{d}{dt} r_E + a_5' r_E$. It is seen that the nonlinear part f can be covered by the control effort u_e, and hence f can be viewed as matched uncertainty.

For a sliding mode controller, its design can be divided into two steps, i.e., design the sliding surface and determine the control law. The sliding surface is usually defined as linear homogenous algebra equations about the plant state. Thus, the sliding surface, combined with linear part of regular form of the system state-space equations, produces stable and desirable system performance simply by using linear system design approaches. For step input, the sliding function is defined as

$$s = c_1(F_{EQ}^c - x_1) + (\dot{F}_{EQ}^c - \dot{x}_1) = c_1(F_{EQ}^c - x_1) - \dot{x}_1 = \mathbf{P}^{\mathrm{T}}(\mathbf{X}_0 - \mathbf{X}) \tag{3.5}$$

where $\mathbf{X}_0 = \begin{bmatrix} F_{EQ}^c & 0 \end{bmatrix}^{\mathrm{T}}$, $\mathbf{P}^{\mathrm{T}} = [c_1 \quad 1]$ and c_1 is a design parameter which can be determined by pole placement method with s=0. It should be noted that the next equal sign of Eqn. 3.5. exists because of step input.

The next step is to determine the control law to drive the state variables of controlled system onto the sliding surface. Lyapunov direct method is employed herein. The Lyapunov function takes the form of

$$v = 0.5s^2 \tag{3.6}$$

The sufficient condition for the sliding surface $\boldsymbol{S}$=0 to occur as $t \to \infty$ is

$$\dot{v} = s\dot{s} = -s\mathbf{P}^{\mathrm{T}}\dot{\mathbf{X}} = -s(\mathbf{P}^{\mathrm{T}}\mathbf{AX} + \mathbf{P}^{\mathrm{T}}\mathbf{B}u_e + \mathbf{P}^{\mathrm{T}}\mathbf{B}f) < 0 \tag{3.7}$$

Essentially, Eqn. 3.7. states that the squared "distance" to the surface, as measured by s^2, decreases with time. Obviously it is desired that system state remains on the surface, once it reaches sliding surface. Then the dynamics on the sliding surface is expressed as

$$\dot{s} = -\mathbf{P}^{\mathrm{T}}\mathbf{AX} - \mathbf{P}^{\mathrm{T}}\mathbf{B}(u_e + f) = 0 \tag{3.8}$$

With the above equation, we obtain the expression for u_e, which is called the equivalent control and denoted by u_{eq}, as

$$u_{eq} = -(\mathbf{P}^{\mathrm{T}}\mathbf{B})^{-1}(\mathbf{P}^{\mathrm{T}}\mathbf{AX} + \mathbf{P}^{\mathrm{T}}\mathbf{B}f) \tag{3.9}$$

It can be interpreted as the continuous control law that will maintain $\dot{s}=0$ if the dynamics, particularly nonlinear part, are exactly known. To attain asymptotic stability, $\dot{v}$ is required to be negative definite by Lyapunov Theorem, i.e., $\dot{v} < 0$ for $s \neq 0$. This can be easily achieved by a continuous control law which takes the form as

$$u_e = u_{eq} + \delta\mathbf{P}^{\mathrm{T}}\mathbf{B}s \tag{3.10}$$

However, the function f denoting system uncertainty is generally unknown, and then the above control can not be implemented in practice. To resolve this problem, the continuous control is replaced by a discontinuous one which is given by

$$u_e = -(\mathbf{P}^{\mathrm{T}}\mathbf{B})^{-1}(\mathbf{P}^{\mathrm{T}}\mathbf{AX} - k\,\mathrm{sgn}(s)) \tag{3.11}$$

in which, sgn(s) is a sign function, i.e., sgn(s)=s/|s|; k is determined by

$$k = -F + \eta \tag{3.12}$$

where η is a strictly positive parameter; F is the bound for $\mathbf{P}^{\mathrm{T}}\mathbf{H}f$, i.e., $\left|\mathbf{P}^{\mathrm{T}}\mathbf{H}f\right| \le F$. It is instantly seen that $\dot{v}$ is negative definite, simply by substituting Eqns. 3.11. and 3.12. into Eqn. 3.7., which gives

$$\dot{v} = -s(k\,\mathrm{sgn}(s) + \mathbf{P}^{\mathrm{T}}\mathbf{B}f) \le -\eta|s| \tag{3.13}$$

To keep the system state on the sliding surface once it is reached, and avoid chattering problem at least theoretically, sgn(0) should take the value such that $\dot{s} = 0$, i.e.,

$$k\,\mathrm{sgn}(0) + \mathbf{P}^{\mathrm{T}}\mathbf{B}f = 0 \tag{3.14}$$

With Eqns. 3.6. and 3.13., it can be proved that the sliding surface s=0 is asymptotically stable. However, the Lypunov theorem can not be applied directly because $\dot{v}$ is not a function only dependent on s, but also dependent on **X**. Utkin (1992) presented an analog to Lyapunov theorem to determine sliding mode domain. For the case in this paper, a much simpler proof is provided in the Appendix.

Notice that state vector **X** includes the first derivatives of the equivalent force F_{EQ}^{m}, which can not be determined through measurement directly. Kalman filter is used herein for state observing; the corresponding mathematical model of the observer is expressed by the state-space equation as

$$\dot{\hat{\mathbf{X}}} = \mathbf{A}\hat{\mathbf{X}} + \mathbf{B}u_e + \mathbf{K}_e(F_{EQ}^{m} - \mathbf{C}\hat{\mathbf{X}}) \tag{3.15}$$

in which $\hat{\mathbf{X}} = [\hat{F}_{EQ}^{m} \quad \dot{\hat{F}}_{EQ}^{m}]^{\mathrm{T}}$ is the observed state vector, and $\mathbf{K}_e$ is the Kalman gain matrix.

Fig. 3.1. shows the block diagram of equivalent force control system with the discontinuous sliding mode controller.

4. CHATTERING PROBLEM AND ITS REMEDY

4.1. Statement of problem

By substituting Eqn. 3.14. into 3.11., the control effort on the sliding surface is obtained as

$$u_e = -(\mathbf{P}^{\mathrm{T}}\mathbf{B})^{-1}(\mathbf{P}^{\mathrm{T}}\mathbf{AX} + \mathbf{P}^{\mathrm{T}}\mathbf{B}f) \tag{4.1}$$

This exactly the same as the equivalent control as shown by Eqn 3.9.. But unfortunately, the value of f is generally unknown even on sliding surface. This means that Eqn 3.8. is not satisfied, i.e., $\dot{s} \neq 0$ on the sliding surface. So when the system state reaches the sliding surface, it will not stay on the surface but tend to cross the surface. But once it goes off the surface when switching in Eqn 3.11. is not infinitely quick, it will again be driven back, according to the stability theorem of sliding mode. Thus the so-called chattering problem is resulted. Because there always exists some delay in the switching mechanism, chattering is evitable in practice of sliding mode control. But chattering effect can be reduced by various approaches, one of which is described below.

4.2. Remedy of chattering

The chattering problem can be eased by adding the second term of the right-hand side of Eqn. 3.10. to 3.11., which results in

$$u_e = -(\mathbf{P}^{\mathrm{T}}\mathbf{B})^{-1}(\mathbf{P}^{\mathrm{T}}\mathbf{A}\mathbf{X} - k\,\mathrm{sgn}(s)) + \delta\mathbf{P}^{\mathrm{T}}\mathbf{B}s \tag{4.2}$$

Substitution of the above into Eqn. 3.8. gives

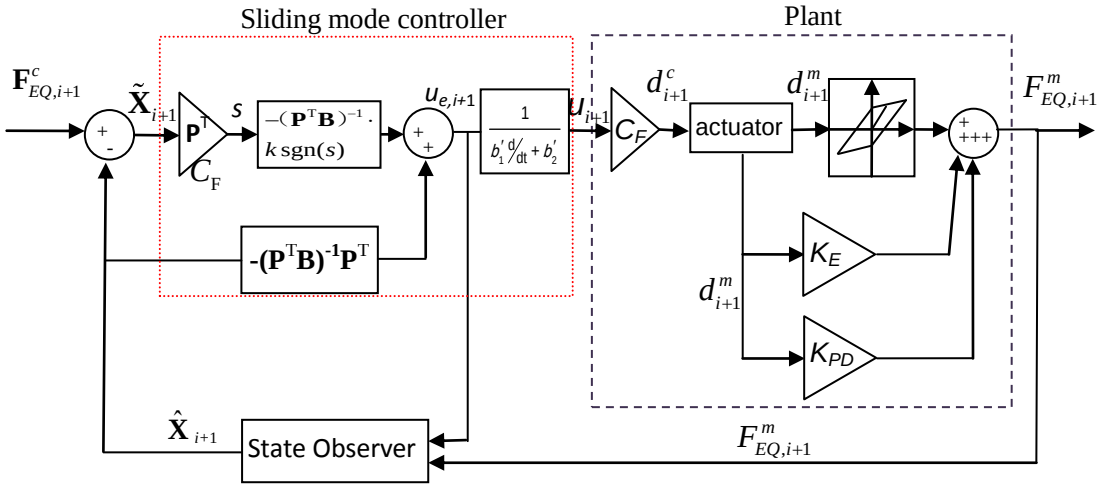

Figure 3.1. Block diagram of EFC with sliding mode controller

$$\dot{s} = k\,\mathrm{sgn}(s) + \mathbf{P}^{\mathrm{T}}\mathbf{B}f + \delta(\mathbf{P}^{\mathrm{T}}\mathbf{B})^2 s \tag{4.3}$$

From the above two equations, we see that the last term of Eqn. 4.2. can be viewed as an extra control effort to drive the system state back to the sliding surface: the farther the state deviates from the surface, the more the control effort is added and the faster the state goes back to the sliding surface. In this way, the deviation from the sliding surface is further restrained and hence the chattering is eased.

Although the chattering can be reduced by Eqn. 4.2., switching in control with the high frequency and large amplitude may bring damage to the hardware of control system. To this end, the boundary layer solution can be used. The control Eqn. 4.2. is replaced by a saturation function which approximates the sgn(*s*) term in a boundary layer of the sliding surface *s*=0, which reads

$$u_e(t) = \begin{cases} -(\mathbf{P}^{\mathrm{T}}\mathbf{B})^{-1}(\mathbf{P}^{\mathrm{T}}\mathbf{A}\mathbf{X} - k\,\mathrm{sgn}(s)) + \delta\mathbf{P}^{\mathrm{T}}\mathbf{B}s; if\ |s| > \Phi \\ -(\mathbf{P}^{\mathrm{T}}\mathbf{B})^{-1}(\mathbf{P}^{\mathrm{T}}\mathbf{A}\mathbf{X} - ks/\Phi) + \delta\mathbf{P}^{\mathrm{T}}\mathbf{B}s; if\ |s| < \Phi \end{cases} \tag{4.4}$$

where Φ is the thickness of the boundary layer of the sliding surface *s*=0. With boundary layer method, the inherent robustness properties of sliding mode control systems are retained, while the undesirable chattering of the sliding mode is eliminated, but the invariance characters of the sliding mode are lost. Therefore, for a realisable control law for servo-hydraulic actuator, a trade-off must be made between control bandwidth and tracking precision [1].

5. NUMERICAL SIMULATION

Numerical simulations are conducted in the time domain with Matlab™. Two examples are presented below: one has a linear spring as the physical substructure and the other has a bilinear buckling-restrained brace (BRB) specimen as the physical substructure.

5.1. Spring specimen

The parameters of a linear SDOF structure adopted for the numerical simulations are: M_N=114.5×10^{3}kg, K_N=2.26×10^{6}N/m, K_E=2.26×10^{6}N/m, C_N=0, and C_E=0, which result in a structural period of 1s. The parameters of actuator are: K_P=3, K_I=3, $K_{\Delta P}$=0.0002,β_E=6.895kN/m, V=0.0069m^3, A_P=0.0248m^2, P=20.34MP$_a$, and k_0=1.0674m^2/s. The integration time interval is 0.02s.

Control law specified in Eqn. 3.10. is employed for this linear case. For simplicity, only two parameters c_1 and δ of sliding mode control are studied in this case. The EF responses of the EFC system subjected to a unit step EF command with different parameter c_1 of sliding function are shown in Fig. 5.1a. From Eqn. 3.5., we see that c_1 determines the speed of x_1 on the sliding surface to approach target F^c_{EQ}; the larger the c_1 is, the quicker the x_1 tracks F^c_{EQ}. This exactly agrees with Fig. 5.1a. Fig. 5.1b. shows the effects of δ. It is see that δ determines the settling time of the system trajectories; the larger δ is, smaller the settling time will be.

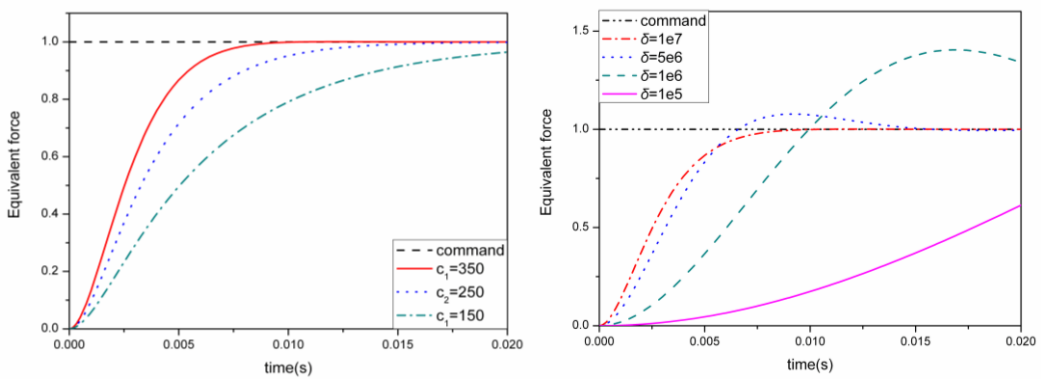

a) Effect of c_1 b) Effect of sliding margin δ

Figure 5.1. Step response with spring specimen

5.2. Bilinear elasto-plastic specimen

The parameters of the structure and actuator are the same as last section except that the experimental substructure is elasto-plastic. The initial stiffness of the specimen K_E=2.26×10^{6}N/m, the yielding displacement is 2mm, the second stiffness coefficient is 5.81%. The integration time interval is 0.01s.

Fig. 5.2. shows the step responses subjected to equivalent force command of 3×10^{4}kN with the discontinuous controller, whose parameters are: c_1=500, δ=0 and k=3×10^{13}. The yielding displacement is deliberately reduced to 0.02mm for the case of step input. The maximum displacement response of the actuator is about 0.026mm, which is larger than the yielding displacement. The maximum of nonlinear part f of system dynamics is about 2.4×10^{10}, which is smaller than k, and this indicates that the Lyapunov stability is satisfied. From Fig. 5.2., we see the obvious chattering of equivalent force response and drive voltage of the servo valve. To ease the chattering, we set δ =10^7. The results are shown in Fig. 5.3., where we clearly see the significant suppression of chattering of the equivalent force as well as the servo-valve voltage. The chattering is further reduced by using boundary layer with the parameter Φ=10^7, which is shown in Fig. 5.4.

The seismic responses subjected to El Centro (NS, 1940) Earthquake are shown in Fig. 5.5.. The parameters of the controller are the same as the case with boundary layer. It is seen that the equivalent force responses track the command well, and the displacement responses match the exact solution very well. The maximum displacement response is nearly 6 mm which is larger than the yield displacement of 2mm, indicating the specimen well goes into nonlinear range.

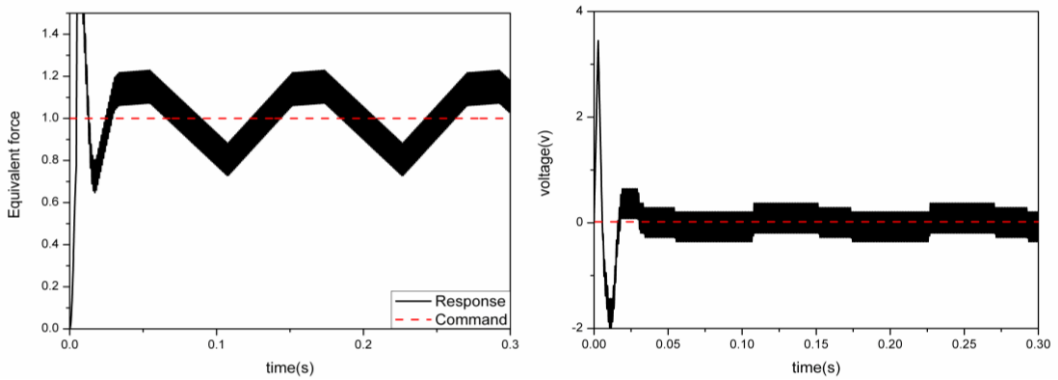

a)Equivalent force response b) Servo-valve voltage

Figure 5.2. Step response with elasto-plastic specimen (δ=0)

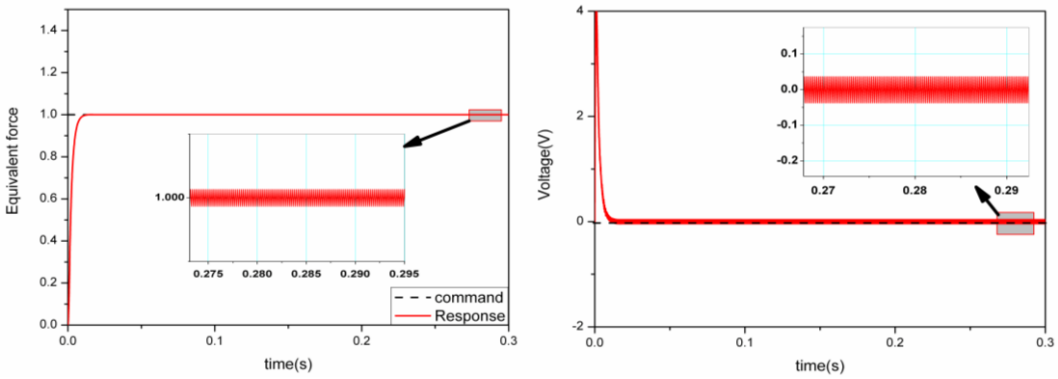

a) Equivalent force response b) Servo-valve voltage

Figure 5.3. Step response with elasto-plastic specimen (δ=10^7)

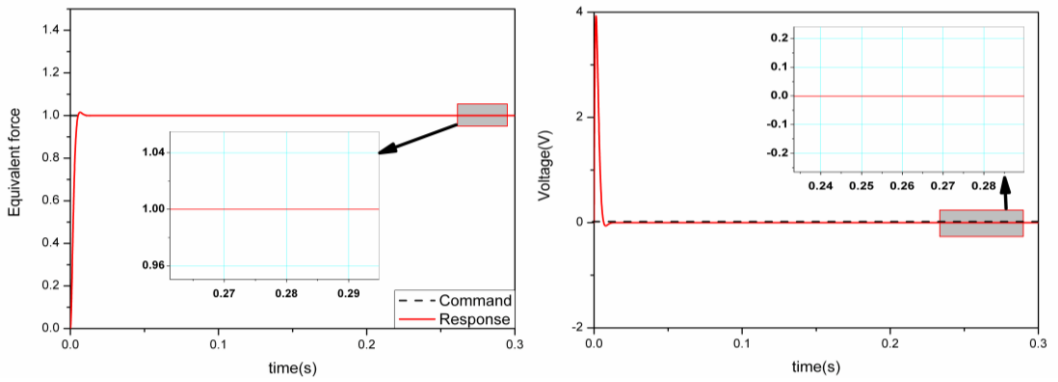

a) Equivalent force response b) Servo-valve voltage

Figure 5.4. Step response with elasto-plastic specimen (Φ=10^7)

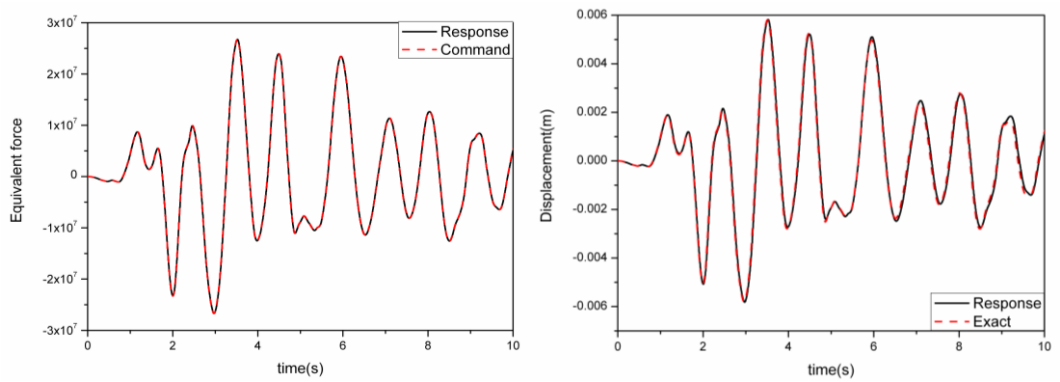

a) Equivalent force b) Displacement

Figure 5.5. Seismic response with elasto-plastic specimen

6. CONCLUSIONS

The sliding mode controller has been proposed for equivalent force control in the hybrid testing with nonlinear specimens. The design of the sliding mode control is presented and the stability is discussed. The effects of key parameters on the performance of sliding mode controller are demonstrated through numerical simulation. The results show the good tracking capacity in spite of strong specimen nonlinearity, and the chattering problem is resolved by choosing proper controller parameters.

ACKNOWLEDGEMENTS

The authors gratefully acknowledge the financial support of the National Science Foundation of China (Grant numbers: 51161120360 and 90715036), the Fundamental Research Funds for the Central Universities (Grant numbers: HIT. BRET2.2010009, HIT.ICRST2010016).

REFERENCES

Bursi O. S., Gonzalez-Buelga A., Vulcan L., Neild S. A. and Wagg D. J.(2008). Novel coupling rosenbrock-based algorithms for real-time dynamic substructure testing. *Earthquake engineering and Structural dynamics* **37:3**, 339-360

Chen C. and Ricles J. M.(2008). Stability analysis of explicit integration algorithms with actuator delay in real -time hybrid testing. *Earthquake Engineering and Structural Dynamics* **37**, 597-613.

Jung R. Y., Shing P. B., Stauffer E. and Thoen B.(2007). Performance of a real-time pseudo dynamic test system Considering Nonlinear Structural Response. *Earthquake Engineering and Structural Dynamics* **36:12**, 1785-1809.

Slotine J. J. and Li W.. Applied nonlinear control. Pearson Education, Prentice-Hall,Inc USA.

Utkin V. I.(1992). Sliding Mode Control in Control and Optimization. Springer-Verlag, Berlin, Germany.

Wang X. Y., Wu B. and Wang Q. Y.(2007). Sliding mode control of real-time substructure testing. *Engineering Mechanics* **24:6**, 174-179.(in Chinese)

Williams, D. M., Williams. M. S. and Blakeborough A.(2001). Numerical modeling of a servo-hydraulic testing system for structures. *Journal of Engineering Mechanics* **127:8**, 816-827.

Wu B., Bao H., Ou J. and Tian S.(2005). Stability and accuracy analysis of central difference method for real -time substructure testing . *Earthquake Engineering and Structural Dynamics* **34:7**, 705-718.

Wu B., Wang Q., Shing P. B. and Ou J. P.(2007). Equivalent force control method for generalized real-time substructure testing with implicite integration. *Earthquake Engineering and Structural Dynamics* **36:9,** 1127-1149.

Wu B., Xu G. and Shing P. B.(2011). Equivalent force control method for real-time testing of nonlinear structures . *Journal of Earthquake Engineering* **15**, 143-164.

Yang J. N., Wu J. C. and Agrawal A. K.(1995). Sliding mode control for nonlinear and hysteretic structures. *Journal of Engineering Mechanics* **121:12**, 1330-1339.

APPENDIX: STABILITY THEOREM OF SLIDING MODE

For convenience of discussion, we list the Lyapunov theorem using the notation for the case in this paper.

Lyapunov theorem for asymptotic stability
If there exist a scalar function $v(s)$ with continuous first partial derivatives such that
(1) $v(s)$ is positive definite
(2) $\dot{v}(s)$ is negative definite
Then the equilibrium point $\mathbf{X}=0$ is asymptoticly stable.

It is important to notice that the Lyapunov function and its time derivative on the above theorem are solely determined by their independent variable *s***.** For the Lyapunov Eqn. 3.6., its time derivative Eqn. 3.7. is not a function of *s*, since it also includes the system variable **X**. To deal with this problem, we need to consider the characteristics of time derivative of sliding function, *i.e.* Inequality 3.13.. Keep this inequality in mind, we prove the asymptotic stability of sliding surface by contradiction.

Since v is lower bounded, *i.e.*, $v \geq 0$, and decreases continually, v tends towards a limit L. Assume that this limit is not zero, *i.e.*, $L>0$. So there exists a range $(-r, r)$ where r is a positive number, which $s(t)$ never enters, since v is continuous about s and $v(0)=0$. Note that $\dot{v}$ is also continuous about s, although $\dot{s}$ is discontinuous on at $s=0$. Then, because $\dot{v}$ is negative definite and $|s| = 2\sqrt{v} \leq 2\sqrt{v_0}$ (v_0 is the initial value of v), $\dot{v}$ must be less than a negative number L_1. This is contradiction, because this would imply that v will reach 0 in a finite time smaller than $v_0/|L_1|$. Therefore, v tends towards 0 and hence so does s.